RESEARCH

Accurate tracking of the mutational landscape of diploid hybrid genomes reveals genetic background effects

Lorenzo Tattini[1], Nicolò Tellini[1], Simone Mozzachiodi[1], Melania D'Angiolo[1], Sophie Loeillet[2], Alain Nicolas[2] and Gianni Liti[1*]

*Correspondence:
gianni.liti@unice.fr
[1]Université Côte d'Azur, CNRS, INSERM, IRCAN, 28 Avenue de Valombrose, 06107 Nice, France
Full list of author information is available at the end of the article

Abstract

Background Genome evolution promotes diversity within a population via mutations, recombination, and whole-genome duplication. However, quantifying precisely these factors in diploid hybrid genomes is challenging. Here we present an integrated experimental and computational workflow to accurately track the mutational landscape of yeast diploid hybrids (MuLoYDH) in terms of single-nucleotide variants, small insertion and deletions, copy-number variants and loss-of-heterozygosity.

Results Haploid *Saccharomyces* parents are combined into diploid hybrids with fully phased genome and controlled levels of heterozygosity. The resulting hybrid represents the ancestral state and is evolved under different laboratory protocols. Variant simulations enable to efficiently integrate competitive and standard mapping, depending on local levels of heterozygosity and read length. Experimental validation in a mutator background proves the high accuracy and resolution of our computational approach. The unbiased estimation of mutation rates across different hybrids reveals striking genetic background effects. Surprisingly, homozygous *S. cerevisiae* shows ∼4-fold higher mutation rate compared to its sister species *S. paradoxus*. In contrast, interspecies hybrids exhibit mutation rate similar to intraspecies hybrids despite 10-fold higher heterozygosity. MuLoYDH reveals that a substantial fraction of the genome (∼200 bp per generation) is continuously shaped by loss-of-heterozygosity and this process is strongly inhibited by high levels of heterozygosity.

Conclusions We report a comprehensive framework for characterizing the mutational spectrum of yeast diploid hybrids with unprecedented resolution, which can be generalised to other genetic systems. Applying MuLoYDH to laboratory-evolved hybrids provides novel quantitative insights into the evolutionary processes that mould yeast genomes.

Keywords: genome evolution; mutation rate; hybrid genomes; heterozygosity; loss-of-heterozygosity; yeast; *S. paradoxus*

Introduction

High-throughput sequencing (HTS) technologies, both short- and long-read, have had a massive impact on genome research, enabling previously unimaginable and detailed dissection of the genomic landscape with outstanding speed and low costs

[1, 2, 3]. The occurrence of variation in sequence, structure, and size of a genome in time is triggered by several factors including DNA mutations, such as single nucleotide variants (SNVs), indels, and copy number variants (CNVs), as well as other structural variants, recombination, and whole-genome duplication. These factors contribute to diversity within a population, translate into quantitative phenotypic variation and may eventually result in speciation. Integrated bioinformatic pipelines, along with high-quality reference assemblies, are fundamental to successfully depict the mutational landscape of genomes [4, 5]. However, *de novo* whole-genome assembly and phasing is still highly challenging and results in incomplete sequences [6, 7]. Thus, the mutational landscape of diploid or polyploid organisms has been characterized through resequencing studies which are based on mapping short reads against a single consensus reference, although the latter misses what defines the genetic identity of one individual [8]. For example, the human genome was assembled using the DNA of ∼50 individuals with just one of them accounting for ∼70% of the sequence, while the yeast reference genome was produced from a single laboratory strain (namely S288C) and its derivatives [9, 10]. Recently, high-quality panels of reference sequences [11, 12, 13] and novel standards for genome assembly [14] have been reported, while graph-based models have been suggested to overcome the limits imposed by reference bias [15, 16, 17]. Nevertheless, using a single reference sequence is a convenient simplification [8] and current technologies are boosting genome quality [18]. Resequencing studies have been proven successful whenever the level of heterozygosity is sufficiently low (e.g. the percentage of polymorphic loci in humans is $< 0.16\%$ [19]) or for homozygous genomes. Yet, mapping against a reference genome raises issues such as (I) the impossibility of probing variation in genomic regions which are not reported in the reference, and (II) no variant phasing information. The latter is a crucial point since current whole-genome sequencing methods do not provide phase information by default. In fact, current phasing methods rely on computational and experimental techniques that require trio data [20] or population-based statistical phasing and long reads to maximise the performance [21].

In addition, natural diploid genomes harbour varying levels of heterozygosity [22]. Analysing diploid hybrid genomes, characterized by high heterozygosity, against a reference poses the problem of spurious read mapping, which in turn may lead to false positive calls of both SNV and indels. High levels of heterozygosity allow for mapping short-read data against *hybrid genome assemblies* obtained by concatenating the two parental subgenomes [23]. This strategy provides direct variant phasing but is risky whenever the number of heterozygous loci is low since it will result in genomic regions characterized by reads with non-unique mapping which in turn will prevent the assessment of small variants (namely SNVs and indels).

Despite these technical difficulties, the study of the role of hybridization in species fitness is an active field of research in evolutionary biology. Unfortunately, notwithstanding the importance of experimental and computational validation of the methods based on HTS data [24, 25, 26], none of the approaches tailored to the analysis of hybrid genomes has been automatized and tested with simulated data [23, 27, 28]. In this context *Saccharomyces cerevisiae*, along with its closely related species, is a leading-edge eukaryotic model system that has long been exploited in genetics, cell

biology and systems biology [29, 30, 31]. The *S. cerevisiae* genome was the first fully sequenced eukaryotic genome [32], and more recently it has also played a crucial role in understanding key principles in evolutionary genomics [33, 34, 35]. Species from the *Saccharomyces* genus have been shown to be prone to intra- and interspecies hybridization [33, 36]. Hybridization occurs ubiquitously with natural hybrids associated with multiple fermenting environments [37, 38, 39, 40]. Outbreeding has also played an important role in shaping *S. cerevisiae* population structure with several groups of strains showing mosaic genomes that result from ancient admixtures of extant lineages [41].

The precise laboratory control of the sexual and asexual phases is a major strength of yeast genetics and enables to combine different species and isolates into designed ancestral diploid hybrids. These diploid hybrids can be evolved under various laboratory protocols such as mutation accumulation lines (MAL) [42, 43, 44, 45], experimental evolution (EE) [46, 47], and return-to-growth (RTG) [27]. RTG experiments generate genome-wide recombinant hybrids characterized by loss-of-heterozygosity (LOH) events. LOHs allow the expression of recessive alleles as well as the formation of new combinations of haplotypes and provide an alternative approach for the analysis of complex traits. EE experiments quantify the preferential accumulation of pre-existing and *de novo* genetic variants that are selected in a controlled environment due to their contribution to organismal fitness. On the contrary, in MAL experiments a bottleneck of one or few individuals is imposed on a population, allowing for non-lethal mutations to accumulate with slight or no filtering by natural selection. Forcing population bottlenecks provides a means to evaluate mutational rates and signatures. Compared to fluctuation assay, MALs yield unbiased genome-wide estimations of the rates but, so far, they have been mostly restricted to laboratory strains, mutator backgrounds, and haploids or homozygous diploids. Thus, a global picture of the mutational landscape, including genetic background effects and a quantitative measure of the impact of LOH, is still missing. In this paper we develop MuLoYDH, a general framework for the comprehensive characterization of the **Mu**tational **L**andscape **o**f **Y**east **D**iploid **H**ybrids. The genetic cross enable to reconstruct a fully phased diploid genome that serves as the ancestral state, which is otherwise impossible to obtain from direct sequencing of hybrid diploids. We generate diploids via designed crosses of haploid parents with fully assembled genomes. After extensive benchmarking against both simulated and experimentally designed diploid *Saccharomyces* hybrids, we use MuLoYDH to accurately characterize intra- and interspecies MALs obtained by crossing domesticated and natural strains. Our strategy reveals striking genetic background effects and quantifies the genome-wide role of LOH in shaping the evolution of hybrid genomes.

Results and discussion

Overview of the MuLoYDH strategy

The MuLoYDH workflow begins with experimentally generating ancestral hybrids by combining two haploid founder strains with fully assembled and annotated genomes. This allows the investigation of the fully phased genome of the derived hybrids. *S. cerevisiae* is an ideal genetic system for this approach since it can be crossed to produce diploid strains with a broad range of heterozygosity (Figure

1a-b). Designed *Saccharomyces* hybrids can range from complete homozygous (0%) when a single strain is used, low heterozygosity (0.1%) derived from strains of the same subpopulation, moderate (0.5-4%) crossing strains from diverged subpopulations and extremely high (8-35%) in interspecies hybrids [22, 23, 11].

The computational strategy implemented in MuLoYDH for tracking the mutational events relies on the presence of single-nucleotide markers (SNMs) between the two parental subgenomes (Additional file 1: Figure S1-S4). Following mitotic hybrid evolution under different defined laboratory conditions (Figure 1c), the corresponding short-read data can be mapped using both *competitive* and standard approach (Figure 1d-e). The former consists in mapping short-read data against the union of the two parental assemblies, whereas the latter refers to mapping against a single parental assembly. The genomic density and distribution of SNMs are fundamental for our purposes since SNMs are probes for LOH detection and, as detailed in the following section, they allow for the identification of small variants (namely, SNVs and indels) with direct phasing from competitive mapping. In addition, SNMs genomic positions are determined from the assemblies and can be used to set up rational quality threshold for LOH detection as well as for filtering *de novo* small variants (see Methods). As expected, the number of SNMs detected aligning *S. paradoxus/S. cerevisiae* assemblies is ∼15-fold higher compared to *S. cerevisiae/S. cerevisiae* assemblies (Table 1). SNMs were classified as lying in collinear regions or lying within structural rearrangements, namely inversions or translocations, and the corresponding fractions were calculated (f_c and f_r, respectively). Using these values we were able to further differentiate the backgrounds beyond the typical heterozygosity measures simply based on sequence divergence. Hybrids derived from the UWOPS03-461.4 and UFRJ50816 show the largest fraction of SNMs within structurally rearranged regions (Figure 1a), consistently with massive genomic rearrangements occurring within these lineages [11].

The SNMs distribution represents a key feature of the hybrid genome and highly impacts the accuracy of *de novo* variants detection. We calculated the low-marker-density-regions (LMDRs) fraction, i.e. the fraction of genomic regions characterized by less than one marker in 300 bp, namely twice the read length of the sequencing experiments discussed in this study (Table 1). Pairs of genomes characterized by a small number of SNMs show higher values of the LMDRs fraction. MuLoYDH can be run in two different settings (collinear/rearranged) exploiting *a priori* knowledge of parental genomes reciprocal structure. In the collinear mode SNMs are determined chromosome-by-chromosome, aligning a chromosome of parent 1 against the corresponding homologous from parent 2, whereas with the rearranged option they are calculated through a single whole-genome alignment of parental assemblies. Running MuLoYDH in collinear mode provides a larger number of SNMs with a uniform distribution along the genome compared to the rearranged mode (Figure S5). Nevertheless, the latter is a general-purpose solution.

The fully phased hybrid genome assembly can be exploited to perform a competitive mapping of the reads obtained from evolved hybrids. This approach, compared to a standard mapping against a single assembly or an unphased reference genome, is expected to provide a larger number of mapped reads in unique regions that belong only to one of the parental assemblies. Indeed, competitive mapping in *S.c.*

hybrids reduced the number of unmapped reads of 8% on average. At the same time, it represents a challenge regarding reads mapping to identical regions within the two parental assemblies. In fact, the fraction of reads showing a mapping quality (MAPQ) value equal to zero [48], thus reflecting non-unique mapping, is also expected to increase as the level of heterozygosity decreases. As expected, the number of reads showing MAPQ = 0 increased in the competitive mapping (43%) with respect to the standard mappings (∼15%) in intraspecies hybrids (see Additional file 2 — Table S1). Nonetheless, the crossing phase does provide the unique opportunity to generate diploid hybrids with phased genome to benchmark computational approaches for studying their evolution. Parents with different genomic features can be chosen, providing a number of potential hybrids that grows quadratically with the number of available parental strains.

Benchmarking MuLoYDH against simulated datasets

Highly similar DNA sequences may occur on different genomic scales, from short stretches (such as homopolymers), to complex events (e.g. segmental duplications), up to chromosome level (i.e. homologous chromosomes) [49]. These repetitive sequences are characterized by nearly 100% sequence identity and represent a major challenge of HTS data analysis [50]. In competitive mapping, the number and distribution of SNMs affect the performance of the small variants calling. As the number of SNMs and the level of heterozygosity decrease, the mapping algorithm produces a progressively increasing number of reads characterized by MAPQ = 0. This in turn may affect the small variants calling algorithm, since reads characterized by ambiguous mapping (i.e. MAPQ = 0) are filtered out. Thus, we investigated the impact of the level of heterozygosity on the performance of MuLoYDH in calling small variants from competitive mapping in simulated genomes (Figure 2a-b). The number of SNMs simulated was chosen to mimic real data (Table 1). As expected, the F_1 score sharply decreases with the number of SNMs. Nevertheless, when the percentage of SNMs is ∼0.5 (as discussed in the following paragraph), the score tends to a value close to 1 (see Additional file 1: Figure S6).

We also compared the performance of competitive and standard mapping in calling small variants simulated in real assemblies as a function of the coverage. This analysis is fundamental since the competitive mapping approach has never been systematically benchmarked on a dataset of simulated variants and inconsistencies among small variants callers have been reported [51, 52, 53, 54, 55, 56]. As expected, using standard mapping for a complete homozygous diploid, the F_1 score increases with coverage showing saturation at 50 x (Figure 2c). On the contrary, calling small variants from heterozygous diploid data mapped with the standard approach provides low F_1 score with few benefits increasing coverage (Figure 2d). This effect is explained by spurious mapping of reads from parent 2 against the assembly of parent 1 (and vice versa) which leads to FPs. In fact, the poor performance can be ascribed to low precision values. Instead, the competitive mapping of heterozygous diploid data (Figure 2e) yields high F_1 score, with a trend similar to the complete homozygous diploid case in the standard mapping. Therefore, competitive mapping can be exploited to call small variants with direct phasing although the overall performance is limited by the number FNs (see recall in Figure 2e). Thus, we included

in MuLoYDH a module that automatically calculates the boundaries of regions characterized by reads with low mapping quality (i.e. MAPQ < 5). These regions are investigated through standard mapping. Although this prevents direct variant phasing, it allows for testing the presence of small variants in the whole accessible regions of the genome.

Moreover, using DBVPG6765/YPS128 hybrid data, we calculated the F_1 score considering only the variants lying within a 65 kb unique region of the Wine/European strain (DBVPG6765) on chromosome XV, derived from horizontal gene transfer from *Torulaspora microellipsoides* [57]. We obtained $F_1 = 0.96$ ($TP = 14$, $FN = 1$, $FP = 0$) on the basis of 15 variants (14 SNV and a 1 bp insertion) combining all the simulated short-read data (20 experiments). Hence, MuLoYDH allows for calling small variants in regions which are not reported in the reference genome.

Another aspect of the small variants calling procedure is whether MuLoYDH can correctly detect and genotype variants in LOH regions. In fact, these regions may carry homozygous variants (occurred before LOH) and heterozygous variants (occurred after LOH). Thus, we compared the genotypes of simulated variants with those reported by MuLoYDH. We obtained an average whole-genome F_1 score of 0.961 ± 0.004 calculated from 4337 variants in 10 replicates. MuLoYDH correctly called and genotyped 1840 variants in the simulated LOH regions (691 homozygous and 1149 heterozygous variants), producing 62 FPs and 207 FNs with, as expected, a larger number of missed events in heterozygous state (121 heterozygous vs 86 homozygous). Remarkably (see Additional file 1: Figure S7), 61 out of 62 FP variants were in variant positions which had been incorrectly genotyped (2 as homozygous and 59 as heterozygous), thus resulting also in a FN. Nevertheless, the genomic positions were correctly called. Among the 61 mis-genotyped FPs, we observed 2 SNVs (one homozygous, one heterozygous). We also detected 58 homozygous mis-genotyped small deletions incorrectly called as heterozygous due to mis-mapping of reads which were not supporting the variant. Finally, only one heterozygous small insertion was incorrectly genotyped as homozygous thus resulting in one FP as well as one FN.

Overall, these results demonstrate that both competitive and standard mapping are required to maximise small variants calling performance. Competitive mapping provides direct variant phasing although it can be used only in regions characterized by a sufficient number of SNMs, while standard mapping is necessary if the local number of SNM is less than 1 in 300 bp.

Applying the MuLoYDH workflow to a mutator background

We next applied MuLoYDH to a SK1/BY hybrid with a mutator background ($tsa1\Delta/tsa1\Delta$) evolved for 25 consecutive single-cell bottlenecks [58]. This hybrid evolved drastically from its ancestral state and accumulated a series of complex LOH events (Figure 3a) and small variants (Figure 3b and Additional file 3: Table S2) providing a challenging testbed for our workflow. A key aspect of LOHs detection is the reliability of small events calls. MuLoYDH provides a robust genotyping approach of SNMs positions determined by aligning the parental assemblies (Figure 3c). Moreover, LOHs are determined exploiting only high-quality SNMs which

are genotyped against both parental assemblies (see Methods). The *tsa1*Δ/*tsa1*Δ hybrid mutator background analysed here accumulated a total of 43 LOH events in ∼500 mitotic generations. These events range from 97 bp to 591 kb, with a median size of 3.2 kb adding up to ∼10% of the genome (∼5 kb per generation), suggesting that the *tsa1*Δ background underwent massive mitotic genomic instability.

We further characterized the mutational spectrum (Figure 3d-e) which included 2 CNVs, 34 SNVs and 1 indel. 24 out of 34 SNVs were phased (12 to SK1, 12 to BY) as well as the only indel detected (to BY chromosome IV). The remaining 10 SNVs were called without phasing. 6 of them were detected in BY LOH regions (4 heterozygous, 2 homozygous), 1 in SK1 LOH regions (homozygous), while the remaining 3 variants were called from standard mapping. 2 phased and 8 unphased variants were tested through Sanger sequencing and all of them were validated as true positives. 6 out of 8 unphased variants were heterozygous, whereas the remaining 2, lying in LOH regions, were genotyped as homozygous and thus further supported the recombination event. We detected a short LOH segment (SK1 allele, start-end distance 741 bp), supported by 4 SNMs (SK1 genotype) bearing tRNA-Ser (AGA). Moreover, the SK1 LOH region lay within a large (> 450 kb, BY genotype) LOH region. The latter carried a validated homozygous missense variant (C → T, YDR484W p.Ser501Phe) that occurred before the large event. Remarkably, one validated intergenic heterozygous variant (Figure 3b, green star) lay within the aforementioned LOH region (BY chromosome IV). Thus, using MuLoYDH we were able to reconstruct the time course of events that occurred in chromosome IV-R: (I) recombination leading to a short LOH, (II) SNV (Figure 3b, yellow star), (III) a large LOH, and (IV) one heterozygous SNV (Figure 3b, right-most green star). Electropherograms, annotated with validated variants, are reported in Additional file 1: Figure S8-S9.

In summary, these results demonstrate that the SNMs quality-filtering approach for LOH detection provides accurate results also for events supported by few markers (Additional file 1: Figure S10). Moreover, validations of *de novo* small variants confirm that combining competitive and standard mapping, along with the filtering strategy based on SNMs quality values, yields reliable calls. The ability to precisely detect all type of mutational events provides an accurate mutational landscape of diploid hybrid genomes.

Evolution through complex copy-number variants

Changes in copy-number, from single gene to whole chromosome events, have been observed in both natural and laboratory evolved strains [59, 60, 61]. MuLoYDH produces CNV calls through Control-FREEC [62] normalizing the read count (RC) signal for GC-content and mappability [63]. The combination of RC signals and B-allele frequencies (BAF) of SNMs, both calculated from standard mapping, shed light on complex events as we demonstrate in an intraspecies UWOPS03-461.4/YPS128 *S. cerevisiae* hybrid evolved via the RTG protocol [27]. A large fraction of the ancestral hybrid genome is non-collinear, due to a massive genome instability occurred in the Malaysian lineage (UWOPS03-461.4). Recombination between non-collinear homologous chromosome potentially results in CNVs. UWOPS03-461.4 chromosome VIII consists of a 350 kb collinear region that spans the centromere and a 390

kb translocation derived from chromosome VII (Figure 4a). The ancestral YPS128 chromosome VIII-R arm bears two regions which were translocated to UWOPS03-461.4 chromosome VII, with the orientation of one segment inverted.

Two double-strand breaks (DSBs) occurred in the UWOPS03-461.4 chromosome VIII (Figure 4a, purple and yellow stars) and were repaired using the homologous YPS128 chromosome VIII region. Chromosome VIII-L arm repair occurred within the collinear region and resulted in a simple LOH event without an associated CNV. The same holds for the collinear region in chromosome VIII-R arm spanning from the DSB to the translocation breakpoint. These regions show BAF $\sim$0 and RC signal fixed at 2 copies (Figure 4b). In contrast, the rearranged chromosome VIII region embedded in the LOH was subjected to CNV, as shown by the RC shift to 3 copies and BAF value $\sim$0.3. The latter supports the presence of a 3-copies region, bearing 2 copies of YPS128 alleles and 1 copy of UWOPS03-461.4 allele.

This complex genomic configuration is further confirmed by the RC signal and the BAF data from chromosome VII, given the loss of the UWOPS03-461.4 translocated region (Figure 4c and Figure S11). Thus, the combination of the exact ancestral chromosomal configuration with our computational framework enables to dissect complex genomic rearrangements.

Mutational rates across different genetic backgrounds

Mutational rates and signatures are key parameters for genome evolution but how these vary across natural genetic backgrounds has remained largely unexplored. We applied the MuLoYDH workflow to investigate the effect of genetic background on mutational rates. We constructed four yeast diploids that enabled multiple comparisons. We used a single *S. cerevisiae* background (DBVPG6765) and crossed it to itself, to a different subpopulation of the same species (*S. cerevisiae* YPS128) and to a different species (*S. paradoxus* N17). This resulted in three diploids with approximately 0%, 0.5% and 15% heterozygosity, that enabled the investigation of the effect of heterozygosity in laboratory evolution experiments. We also generated a complete homozygous *S. paradoxus* N17 diploid to compare *S. cerevisiae* to its closely related species. We performed MALs experiments using 8 replicated lines for each of the 4 diploids subjected to 120 consecutive single-cell bottlenecks. The corresponding number of generations was estimated measuring the colony cell population size, observing minimal differences between the four hybrids (Table 2). Mutation rates of SNVs, indels, CNVs and LOHs (the latter only for the heterozygous hybrids) were derived and revealed surprising quantitative differences (see Additional files 4-7: Tables S3-S6 for a list of all the variants). First, the SNVs mutation rate in *S. cerevisiae* was very close to previous reports estimated using laboratory strains indicating no major differences in our Wine/European background [45]. Surprisingly, we observed a 4-fold lower (p-value < 0.0005, Welch's t-test) mutation rate in *S. paradoxus* (95% CI t-distribution: $[3.39, 11.1]\cdot 10^{-11}$ bp^{-1}) compared to *S. cerevisiae* (95% CI t-distribution: $[1.98, 3.67] \cdot 10^{-10}$ bp^{-1}). The same trend was detected for indels and CNVs. The lower mutation rate of *S. paradoxus* might have contributed to the slower evolution of this species compared to *S. cerevisiae*, which is visible from the overall branch length differences observed between the two species since the split from their last common ancestor [11, 64]. The SNVs mutation rate in the

two heterozygous hybrids is also slightly different (p-value = 0.016, Welch's t-test) with the highly heterozygous interspecies hybrid DBVPG6765/N17 showing higher rate (95% CI t-distribution: $[1.73, 2.74] \cdot 10^{-10}$ bp^{-1}) compared to the intraspecies hybrid YPS128/DBVPG6765 (95% CI t-distribution: $[1.09, 1.89] \cdot 10^{-10}$ bp^{-1}). We also compared the mutation rates of different classes of variants for both the intra- and interspecies hybrids. As reported in Table 2, the mutation rate calculated for indels and CNVs was one order of magnitude smaller compared to SNVs and LOHs.

The two heterozygous hybrids showed a substantial difference in term of LOH rates. Mitotic recombination events are rare and usually require a selection method to be detected [65]. Nevertheless, given the large number of generations performed in our study, we were able to observe a relatively large number of LOH events in hybrids. Moreover, being our approach based on both parental assemblies, we were able to call LOHs without filtering out small events using an arbitrary threshold based on the number of supporting markers [27, 28]. This aspect is crucial since we aim at comparing LOH rates in *S. cerevisiae/S. cerevisiae* and *S. paradoxus/S. cerevisiae* crosses. Intraspecies hybrids showed a larger number of LOHs (114) compared to the interspecies hybrids (53) along with (I) a 5-fold higher fraction of genome in LOH (0.02 ± 0.01 and 0.004 ± 0.007, respectively), and (II) a larger number of large events (> 25 kb), namely 3 and 0.4 on average per sample (Additional file 4: Table S3). Thus, the mitotic recombination rate was higher in *S. cerevisiae/S. cerevisiae* compared to *S. paradoxus/S. cerevisiae* crosses (p-value < 0.001, Welch's t-test). Heatmaps of the detected events are reported in Additional file 1 (Figure S12) and the corresponding LOH segments are reported in Additional file 8. Overall, these results provide a quantitative genome-wide measure of the importance of LOHs in shaping polymorphisms patterns in diploid hybrid genomes and how this process is strongly inhibited by very high heterozygosity.

Conclusions

In this study, we presented a novel experimental/computational approach for tracking the mutational landscape of yeast hybrid genomes. Haploid parents with varying levels of heterozygosity were combined into a wide range of diploid hybrids which were evolved in different laboratory settings. MuLoYDH was developed to take advantage of the fully phased diploid genome assembly as ancestral state and Illumina short reads from the evolved hybrids. The presence of single-nucleotide markers provided a reliable quality threshold for filtering *de novo* small variants, thus bypassing the need of multiple hard filters. Moreover, it enabled direct phasing of *de novo* SNVs, indels and CNVs as well as precise characterization of LOHs. Our method was designed to yield a quantitative measure of the fraction of the genome which cannot be probed for direct phasing through competitive mapping and to perform variant calling in these regions by means of a standard approach based on a single reference. It was devised to resolve the drawbacks of using a single consensus reference genome: (I) spurious read mapping, which may lead to false positive calls of both SNV and indels, (II) the impossibility of probing variation in genomic regions which are not reported in the reference, as well as (III) impracticable direct variant phasing. The latter has been the focus of several computational studies (based on a consensus reference) but solving exactly the problem is demanding since

it is a NP-hard problem [7]. Extensive validation of the variants detected by MuLoYDH in a mutator MAL showed that it can be used to trace the time course of mutation occurrence with direct phasing information. While several studies focused on the mutation rates in haploid and complete homozygous diploid *S.c.* laboratory strains [42, 43, 44, 45], we used MuLoYDH to track the mutational landscape of 4 MALs with varying levels of heterozygosity, providing the first measurement of mutation rates in *S. paradoxus*. Surprisingly, we observed low mutation rates in natural N17 *S. paradoxus* homozygous diploids compared to DBVPG6765 *S. cerevisiae*. Moreover, we were able to compare LOH rates in inter- and intraspecies hybrids. The SNVs and LOHs mutation rates demonstrate that these classes of variants, loss-of-heterozygosity in particular, are major sources of genomic variability and play a key role in genome evolution. Our study can be extended to other *Saccharomyces* hybrids, encompassing the whole spectrum of heterozygosity, and to complex genomes bearing structural rearrangements or characterized by ploidy > 2 [22, 66]. Remarkably, as the number of available annotated assemblies increases, the number of potential hybrids grows quadratically and the hybridization process can be easily automated [67].

Resequencing studies show intrinsic limits, particularly in the context of hybrid genomes. Variation graphs will help overcoming this deficiency although they will require extensive efforts to exhaustively support the shift to the new graph-based paradigm [8, 17]. Long-read sequencing is a valuable approach to provide novel reference genomes by means of *de novo* assembly. The availability of novel reference genomes opens new perspectives on resequencing approaches, allowing for investigations of the genomic mutational landscape with unprecedented resolution via short-read experiments. Still, current methods for assembling and phasing diploid genomes are costly and yield to limited contiguity [7]. Recently, long-read sequencing has been exploited to evaluate the performance of small variants callers through a synthetic-diploid benchmark [68]. Here we extended the benefits of long-read sequencing beyond synthetic diploids to evolved *Saccharomyces* hybrids. MuLoYDH provides a unified method for the systematic analysis of genomic variants in yeast diploid hybrids designed for studying genome dynamics and may be extended to non-clonal sequencing data. Moreover, as the sequencing technologies provide reads more and more accurate and long, they will soon allow to produce fully assembled and phased natural hybrid diploid genomes. At this stage, the initial experimental approach implemented here will be possibly bypassed while the computational strategy developed in MuLoYDH will be readily appropriate for the application to natural genomes.

Methods

Simulated data

Simulations of hybrid genomes with varying levels of heterozygosity. Diploid genomes with varying levels of heterozygosity were simulated by custom R scripts, modifying the number of SNMs between the two parental subgenomes. Given two input assemblies (DBVPG6765 and YPS128), SNM positions were determined by MUMmer (NUCmer) [69]. Decreasing values of SNMs percentage were obtained by progressively replacing the allele of assembly 1 with the corresponding allele, as determined by NUCmer, of assembly 2 in known positions. The substitution step was

repeated in order to provide different levels of SNMs (0.5%, 0.1%, 0.05%, 0.01%, 0.005%, 0.001%). For each SNMs value, 3 replicated assemblies were simulated.

Simulations of short reads for heterozygous hybrids. Simulated paired-end short reads were generated using the DWGSIM package [24]. In order to produce simulated short-read data from genome assemblies, two input reference assemblies were concatenated to produce a single multi-FASTA, which was sampled to build simulated paired-end (150 bp, insert size 500 bp) Illumina experiments with different coverage levels (10, 50, 100, 150 x). The mutation rate was set to 10^{-5} with the purpose of balancing a relevant number of small variants (∼240 per genome) with the storage and the computational resources required for data processing. All the simulations were performed using the following parameters: 0.01 error rate for both forward and reverse read, and 0.1 indel/SNV ratio (according to estimations from real Illumina data). Base quality parameters were set according to the real data reported in this paper. Each simulation was performed in 5 replicates. The command line is reported in Additional file 1.

Simulations of short reads for hybrids bearing LOH regions. Short-read data of DBVPG6765/YPS128 hybrids bearing LOHs (with DBVPG6765 alleles) were obtained using DWGSIM with heterozygous genomes with the exception of chromosome I for which two copies of the FASTA sequence of DBVPG6765 were used as input. In order to have a robust statistic, the mutation rate was set to 10^{-3} for chromosome I and to 10^{-5} for all the other chromosomes. The average coverage was set to 50 x on the basis of the short-read simulations from real assemblies. 10 replicates were produced. All the other parameters were set as described above. Overall, we simulated 2304 variants in heterozygous regions of the genome and 2081 in LOH regions (787 homozygous and 1294 heterozygous).

Simulations of short reads from simulated hybrid genomes. Short reads from simulated hybrid genomes with different levels of heterozygosity (as described above) were obtained using DWGSIM with the parameters reported above. The average coverage was set at 50 x on the basis of the short-read simulations from real assemblies. Each simulation was performed in 3 replicates.

Performance of small variants calling. Given a set of relevant elements (i.e. the simulated variants) and a set of selected elements (i.e. the called variants) we classified each element (namely each variant) as true positive (TP), false positive (FP) or false negative (FN). We calculated precision as $P = TP/(TP + FP)$ and recall as $R = TP/(TP + FN)$. The performance of the small variants calling was quantified in terms of the F_1 score which was calculated as the harmonic mean of (P) and (R) according to: $F_1 = 2 \cdot (P \cdot R)/(P + R)$. All the calculations were performed after filtering out polymorphic positions (SNMs and indels) determined by NUCmer as described below. In order to fairly compare competitive and standard mapping, the latter approach was run using a control sample for variant subtraction. This allowed for filtering out polymorphic positions (SNMs and indels) which could not be detected by NUCmer.

Experimental data

Dataset 1 comprises a mutation accumulation line data from a mutator SK1/BY hybrid (*MATa/MATα; ARG4/arg4-nsp,bgl; his3Δ1/HIS3; leu2Δ0/leu2; met15Δ0/MET15; ura3Δ0/ura3; tsa1::KanMX/tsa1::KanMX*) [70]. This dataset was analyzed using the SK1 and S288C assemblies included in MuLoYDH.

Dataset 2 consists of the UWOPS03-461.4/YPS128 hybrid (low sequence divergence; non-collinear genomes with chromosomal rearrangements) evolved under the RTG protocol.

Dataset 3 is composed by MALs from four distinct diploid backgrounds: N17/DBVPG6765, YPS128/DBVPG6765, N17/N17 and DBVPG6765/DBVPG6765. Each MAL consisted of eight independently propagated lines. *S. cerevisiae* DBVPG6765 homozygous diploids (*MATa/MATα, ho::HygMX/ho::HygMX, ura3::KanMX/ura3::KanMX, LYS2/lys2::URA3*) were derived from the Wine/European subpopulation. *S. paradoxus* N17 homozygous diploids (*MATa/MATα, ho::HygMX/ho::HygMX, ura3::KanMX/ura3::KanMX, LYS2/lys2::URA3*) were derived from the European subpopulation. YPS128/DBVPG6765 *S. cerevisiae* intraspecies hybrids (*MATa/MATα, ho::HygMX/ho::HygMX, ura3::KanMX/ura3::KanMX, LYS2/lys2::URA3*) were obtained by mating of North American (YPS128) and Wine/European (DBVPG6765) haploid strains. N17/DBVPG6765 interspecies hybrids (*MATa/MATα, ho::HygMX/ho::HygMX, ura3::KanMX/ura3::KanMX, LYS2/lys2::URA3*) were obtained by mating a *S. paradoxus* haploid strain from the European subpopulation (N17) and a *S. cerevisiae* haploid strain from the Wine/European subpopulation (DBVPG6765). Eight parallel mutation accumulation lines were propagated from each parental background on YPD solid medium (1% yeast extract, 2% peptone, 2% dextrose, 2% agar) and passed through a single cell bottleneck every ∼48 hours (∼20 generations) at 30 °C, for a total of 120 bottlenecks (∼2400 generations). At each single cell bottleneck, a random colony was streaked to isolate the next single colony. To avoid any involuntary selection, at each streak, the closest colony to the center of the plate was picked, independently of its size. To determine the number of generations passed after 48 h, three colonies for each parental background were independently resuspended in 100 μl of sterile water and serially diluted. 20 μl of each dilution were plated on solid YPD medium and grown for ∼48 h at 30 °C. The number of colonies was manually counted in the plate with suitable dilution and the number of generations (G) was estimated according to: $G = log_2(n \cdot d)$, where n is the number of cells counted on the plate and d is the corresponding dilution factor. The results are reported in Additional file 9: Table S8. After 120 single cell bottlenecks, cells were inoculated in 5 ml liquid YPD cultures and grown overnight at 30 °C in a shaking incubator. DNA was extracted using "Yeast Masterpure kit" (Epicentre, USA) following the manufacturer's instructions.

Sequencing

Illumina paired-end libraries (2 x 150 bp) were prepared according to manufacturer's standard protocols and sequenced with an HiSeq 2500 instrument, at the NGS platform of Institut Curie. Coverage statistics are reported in Additional file 10: Table S9.

Experimental validation of variants

9 SNVs variants from the SK1/BY hybrid were validated by Sanger sequencing. SNVs were randomly selected to avoid any bias. A pair of primers (upstream and downstream) was designed for each SNV using Unipro UGENE [71]. PCR products were sequenced by Eurofins Genomics^{TM}. The presence and the genotype of the variants were checked by visual inspection of the electropherograms.

Data analysis

Assembly correction. The assembly of *S. paradoxus* strain N17 was obtained correcting the genome sequence of its close relative CBS432, for which a complete assembly is available [11, 41]. The correction was performed using Pilon [72] with short-read data from Illumina sequencing of a diploid homozygous N17 sample. The command line is reported in Additional file 1.

MuLoYDH general description. The MuLoYDH pipeline requires as input: (1) a dataset of short-read sequencing experiments from yeast diploid hybrids and (2) the two parental genomes which were used to produce the hybrids in FASTA format as well as the corresponding annotations in the "general feature format" (GFF) (see Additional file 1: Figure S15). Reads from hybrid data are mapped against the assemblies of the two parental genomes separately (standard mappings) and against the union of the two aforementioned assemblies (namely a multi-FASTA obtained concatenating the two original assemblies) to produce the competitive mappings (Figure 1d-f). In the latter case, reads from parent 1 are expected to map to the assembly of parent 1 on the basis of the presence of single-nucleotide markers. Conversely, reads from parent 2 are expected to map to the assembly of parent 2. Standard mappings are used to determine the presence of CNVs. The latter are also exploited to discriminate LOHs due to recombination from those resulting by deletion of one parental allele. The SNMs between the parental assemblies are determined by the NUCmer algorithm and are exploited to map LOH segments. SNMs are genotyped from standard mappings. *De novo* small variants are determined from both competitive and standard mappings. Competitive mapping allows for direct variant phasing in heterozygous regions. Variant calling from competitive mapping is performed is performed setting ploidy = 1 in heterozygous regions and ploidy = 2 in LOH blocks. Regions characterized by reads with low mapping quality (MAPQ < 5 in the competitive mapping) are assessed from standard mapping using arbitrarily the assembly from parent 1. All the scripts described in the following sections are embedded in MuLoYDH.

Quality check, mapping, mapping refinement and coverage calculation. Data quality is assessed by FastQC version 0.11.4. Competitive and standard mappings of Illumina reads are performed with BWA version 0.7.12-r1039 using the MEM algorithm [73]. Assemblies can be downloaded from the "Population-level Yeast Reference Genomes" website (https://yjx1217.github.io/Yeast_PacBio_2016/welcome/). Duplicates are removed by SAMtools 1.3.1 (using HTSlib 1.3.1). Depth of coverage is calculated with SAMtools (depth) and awk scripts. Additional file 11: Table S10 reports the coverage calculated for all the samples analysed in this study.

Determination of single-nucleotide marker positions. Single-nucleotide marker positions are determined through the NUCmer algorithm (MUMmer version 3) [with show-snps -ClrT] [69]. In order to obtain reliable SNM positions and take advantage of the "seed and extend" strategy of the algorithm, SNMs are calculated in both direct (assembly 1 vs assembly 2) and reverse (assembly 2 vs assembly 1) ways. The intersection of the two sets is retained for LOH detection and to calculate statistics.

Classification of single-nucleotide markers. SNMs are classified as lying in collinear or rearranged regions as determined by MUMmer and custom R scripts. The fraction of SNMs within collinear regions (f_c) is calculated as $f_c = 1 - f_r$, where f_r is the fraction of SNMs lying within rearranged regions, namely inter- and intra-chromosome inversions and translocations.

SNMs genotyping, small variants calling, annotation and filtering. SNMs calling and genotyping is performed using SAMtools (mpileup) [-u -min-MQ5 –skip-indels -E] and BCFtools (call) [-c -Oz] from standard mappings. SNMs are quality filtered removing those with quality $< (\mu - \sigma)$, where μ is the sample SNM mean quality value and σ is the corresponding standard deviation.

The strategy implemented in MuLoYDH for calling small variants relies on a stringent procedure to limit the number of false positives and keep the number of false negatives as low as possible. Thus, in order to balance performance (in terms of F_1 score) and both the required computational resources and running time, two general-purpose small variants callers are implemented in MuLoYDH. SNVs and indels are called with: (i) SAMtools (mpileup) [-u -min-MQ5 -E] and BCFtools (call) [-c -Oz], and (ii) FreeBayes [74, 75]. Only variants called by both are retained. Both callers are exploited using competitive and standard mappings as described above. Regions characterized by reads with MAPQ < 5 in competitive mappings are determined by custom R scripts, bash scripts and BEDTools [76]). Parental and control hybrid variation is subtracted from hybrids data using custom bash scripts, VCFtools [77] and tabix [78]. The resulting variants are quality filtered masking those characterized by quality $< (\mu - \sigma)$, where μ is the sample SNMs mean quality value and σ is the corresponding standard deviation. Variants bearing SNM alleles are filtered out, while those lying within (sub)telomeric regions are masked. Small variants are annotated by means of SnpEff [79]. SnpEff database is built exploiting the annotations from the "Population-level Yeast Reference Genomes" website.

Copy-number variants calling and annotation. Copy-number variants are estimated by means of Control-FREEC with no matched normal samples, using standard mappings against both parental genomes [62]. Read-count data are normalized by GC-content and mappability. Mappability is calculated with GEM-mappability [80]. Results are annotated with p-values calculated with both Kolmogorov-Smirnov and Wilcoxon Rank-Sum tests.

Loss-of-heterozygosity detection and annotation, calculation of low-marker-density-regions. Loss-of-heterozygosity regions are determined and annotated using custom R scripts. Considering standard mappings of each hybrid against both parental

assemblies, SNM positions characterized by non-matching genotype or alternate allele are filtered out, as well as multiallelic sites. Furthermore, SNMs involved in large deletions, as predicted by Control-FREEC, are masked. Finally, stretches of consecutive SNM positions are grouped in LOH regions. LOH regions are annotated as terminal/interstitial as well as with genomic features embedded and those potentially involved in breakpoints. Annotation is performed based on the genomic features downloaded from the "Population-level Yeast Reference Genomes" website. Regions characterized by less than one SNM in 300 bp are calculated using custom R scripts.

Calculation of low-marker-density-regions. Regions characterized by less than one SNM in 300 bp are calculated using custom R scripts which are embedded in the MuLoYDH pipeline.

Platform. MuLoYDH was developed, tested and optimized using a Linux environment (OS openSUSE 13.2 x86_64), equipped with 64 Intel® Xeon® CPUs (E7-4820 @ 2.00 GHz).

Variants filtering in MALs and calculation of mutation rates. Small variants in DBVPG6044 and N17 homozygous backgrounds were quality-filtered on the basis of the values calculated from the SNMs of DBVPG6044/N17 hybrids as described above. All the small variants called by MuLoYDH were checked by visual inspection using IGV [81]. We also refined the lists of called CNVs by visual inspection in order to (I) avoid FPs due to small events which were not called in the control sample and (II) merge large events (e.g. aneuploidies) which were called as multiple shorter events. For each sample, we calculated the mutation rates dividing the number of variants detected and verified by visual inspection for number of generations calculated and for the length of the corresponding genome. Subtelomeric and telomeric regions were excluded from the calculation of small variants to avoid errors due to repeated regions.

Analysis of homozygous diploids. In order to analyze data from homozygous diploids, we set up a dedicated pipeline which is described in the following section. Reads from homozygous diploids were mapped against the proper assembly with BWA version 0.7.12-r1039 (MEM algorithm). Assemblies were downloaded from the "Population-level Yeast Reference Genomes" website. Duplicates were removed by means of SAMtools 1.3.1 (using HTSlib 1.3.1). Depth of coverage was calculated with SAMtools (depth) and awk scripts. Following duplicates removal, small variants were called with SAMtools and FreeBayes. The intersection of their outputs was retained and variants reported in control samples were removed. Small variants were annotated by means of SnpEff. SnpEff database was built exploiting the annotation data downloaded from the "Population-level Yeast Reference Genomes" website. The presence of copy-number variants was assessed by means of Control-FREEC with no matched normal samples. Read-count data were normalized by GC-content and mappability, while the latter was calculated by means of GEM-mappability. Results were annotated with p-values calculated with both Kolmogorov-Smirnov and Wilcoxon Rank-Sum tests.

Supporting Information

Competing interests

The authors declare that they have no competing interests.

Author contributions

LT: wrote the paper, implemented computational methods, performed simulations, analyzed data; NT: analyzed data, performed simulations; SM: tested computational methods, performed experimental validations; MDA: performed MAL experiments; SL: conducted the experiments; AN: designed the study; GL: wrote the paper, designed the study.

Acknowledgements

We thank Matteo De Chiara for discussions, Olivier Croce for technical support, Agnès Llored for experimental help, Gilles Fischer for critical reading of the manuscript, and the NGS platform of the Institut Curie for NGS sequencing. This work was supported by: (A) Agence Nationale de la Recherche (ANR-11-LABX-0028-01, ANR-13-BSV6-0006-01 and ANR-16-CE12-0019) and Fondation ARC pour la Recherche sur le Cancer (PJA20151203273), and (B) French government, through the UCAJEDI Investments in the Future project managed by the National Research Agency (ANR) with the reference number ANR-15-IDEX-01.

Author details

[1]Université Côte d'Azur, CNRS, INSERM, IRCAN, 28 Avenue de Valombrose, 06107 Nice, France. [2]Institut Curie, Paris Cedex 05, Paris, France.

References

1. Goodwin, S., McPherson, J.D., McCombie, W.R.: Coming of age: ten years of next-generation sequencing technologies. Nat Rev Genet **17**(6), 333–51 (2016). doi:10.1038/nrg.2016.49
2. Stephens, Z.D., Lee, S.Y., Faghri, F., Campbell, R.H., Zhai, C., Efron, M.J., Iyer, R., Schatz, M.C., Sinha, S., Robinson, G.E.: Big data: Astronomical or genomical? PLoS Biol **13**(7), 1002195 (2015). doi:10.1371/journal.pbio.1002195
3. Magi, A., Pisanti, N., Tattini, L.: The source of the data flood: Sequencing technologies. Ercim News (104), 25–26 (2016). Special Issue Ercim: Tackling Big Data in the Life Sciences
4. Magi, A., D'Aurizio, R., Palombo, F., Cifola, I., Tattini, L., Semeraro, R., Pippucci, T., Giusti, B., Romeo, G., Abbate, R., Gensini, G.F.: Characterization and identification of hidden rare variants in the human genome. BMC Genomics **16**, 340 (2015). doi:10.1186/s12864-015-1481-9
5. Wong, K.H.Y., Levy-Sakin, M., Kwok, P.-Y.: De novo human genome assemblies reveal spectrum of alternative haplotypes in diverse populations. Nat Commun **9**(1), 3040 (2018). doi:10.1038/s41467-018-05513-w
6. Garg, S., Rautiainen, M., Novak, A.M., Garrison, E., Durbin, R., Marschall, T.: A graph-based approach to diploid genome assembly. Bioinformatics **34**(13), 105–114 (2018). doi:10.1093/bioinformatics/bty279
7. Sedlazeck, F.J., Lee, H., Darby, C.A., Schatz, M.C.: Piercing the dark matter: bioinformatics of long-range sequencing and mapping. Nat Rev Genet **19**(6), 329–346 (2018). doi:10.1038/s41576-018-0003-4
8. Church, D.M.: Genomes for all. Nat Biotechnol **36**(9), 815–816 (2018). doi:10.1038/nbt.4244
9. Cherry, J.M., Hong, E.L., Amundsen, C., Balakrishnan, R., Binkley, G., Chan, E.T., Christie, K.R., Costanzo, M.C., Dwight, S.S., Engel, S.R., Fisk, D.G., Hirschman, J.E., Hitz, B.C., Karra, K., Krieger, C.J., Miyasato, S.R., Nash, R.S., Park, J., Skrzypek, M.S., Simison, M., Weng, S., Wong, E.D.: Saccharomyces genome database: the genomics resource of budding yeast. Nucleic Acids Res **40**(Database issue), 700–5 (2012). doi:10.1093/nar/gkr1029
10. Engel, S.R., Dietrich, F.S., Fisk, D.G., Binkley, G., Balakrishnan, R., Costanzo, M.C., Dwight, S.S., Hitz, B.C., Karra, K., Nash, R.S., Weng, S., Wong, E.D., Lloyd, P., Skrzypek, M.S., Miyasato, S.R., Simison, M., Cherry, J.M.: The reference genome sequence of saccharomyces cerevisiae: then and now. G3 (Bethesda) **4**(3), 389–98 (2014). doi:10.1534/g3.113.008995
11. Yue, J.-X., Li, J., Aigrain, L., Hallin, J., Persson, K., Oliver, K., Bergström, A., Coupland, P., Warringer, J., Lagomarsino, M.C., Fischer, G., Durbin, R., Liti, G.: Contrasting evolutionary genome dynamics between domesticated and wild yeasts. Nat Genet **49**(6), 913–924 (2017). doi:10.1038/ng.3847
12. Maretty, L., Jensen, J.M., Petersen, B., Sibbesen, J.A., Liu, S., Villesen, P., Skov, L., Belling, K., Theil Have, C., Izarzugaza, J.M.G., Grosjean, M., Bork-Jensen, J., Grove, J., Als, T.D., Huang, S., Chang, Y., Xu, R., Ye, W., Rao, J., Guo, X., Sun, J., Cao, H., Ye, C., van Beusekom, J., Espeseth, T., Flindt, E., Friborg, R.M., Halager, A.E., Le Hellard, S., Hultman, C.M., Lescai, F., Li, S., Lund, O., Løngren, P., Mailund, T., Matey-Hernandez, M.L., Mors, O., Pedersen, C.N.S., Sicheritz-Pontén, T., Sullivan, P., Syed, A., Westergaard, D., Yadav, R., Li, N., Xu, X., Hansen, T., Krogh, A., Bolund, L., Sørensen, T.I.A., Pedersen, O., Gupta, R., Rasmussen, S., Besenbacher, S., Børglum, A.D., Wang, J., Eiberg, H., Kristiansen, K., Brunak, S., Schierup, M.H.: Sequencing and de novo assembly of 150 genomes from denmark as a population reference. Nature **548**(7665), 87–91 (2017). doi:10.1038/nature23264
13. Ameur, A., Che, H., Martin, M., Bunikis, I., Dahlberg, J., Höijer, I., Häggqvist, S., Vezzi, F., Nordlund, J., Olason, P., Feuk, L., Gyllensten, U.: De novo assembly of two swedish genomes reveals missing segments from the human grch38 reference and improves variant calling of population-scale sequencing data. Genes (Basel) **9**(10) (2018). doi:10.3390/genes9100486
14. Editorial: A reference standard for genome biology. Nat Biotechnol **36**(12), 1121 (2018). doi:10.1038/nbt.4318
15. Eggertsson, H.P., Jonsson, H., Kristmundsdottir, S., Hjartarson, E., Kehr, B., Masson, G., Zink, F., Hjorleifsson, K.E., Jonasdottir, A., Jonasdottir, A., Jonsdottir, I., Gudbjartsson, D.F., Melsted, P., Stefansson, K., Halldorsson, B.V.: Graphtyper enables population-scale genotyping using pangenome graphs. Nat Genet **49**(11), 1654–1660 (2017). doi:10.1038/ng.3964

16. Paten, B., Novak, A.M., Eizenga, J.M., Garrison, E.: Genome graphs and the evolution of genome inference. Genome Res **27**(5), 665–676 (2017). doi:10.1101/gr.214155.116
17. Garrison, E., Sirén, J., Novak, A.M., Hickey, G., Eizenga, J.M., Dawson, E.T., Jones, W., Garg, S., Markello, C., Lin, M.F., Paten, B., Durbin, R.: Variation graph toolkit improves read mapping by representing genetic variation in the reference. Nat Biotechnol **36**(9), 875–879 (2018). doi:10.1038/nbt.4227
18. Pennisi, E.: New technologies boost genome quality. Science **357**(6346), 10–11 (2017). doi:10.1126/science.357.6346.10
19. 1000 Genomes Project Consortium, Auton, A., Brooks, L.D., Durbin, R.M., Garrison, E.P., Kang, H.M., Korbel, J.O., Marchini, J.L., McCarthy, S., McVean, G.A., Abecasis, G.R.: A global reference for human genetic variation. Nature **526**(7571), 68–74 (2015). doi:10.1038/nature15393
20. Koren, S., Rhie, A., Walenz, B.P., Dilthey, A.T., Bickhart, D.M., Kingan, S.B., Hiendleder, S., Williams, J.L., Smith, T.P.L., Phillippy, A.M.: De novo assembly of haplotype-resolved genomes with trio binning. Nat Biotechnol (2018). doi:10.1038/nbt.4277
21. Choi, Y., Chan, A.P., Kirkness, E., Telenti, A., Schork, N.J.: Comparison of phasing strategies for whole human genomes. PLoS Genet **14**(4), 1007308 (2018). doi:10.1371/journal.pgen.1007308
22. Peter, J., De Chiara, M., Friedrich, A., Yue, J.-X., Pflieger, D., Bergström, A., Sigwalt, A., Barre, B., Freel, K., Llored, A., Cruaud, C., Labadie, K., Aury, J.-M., Istace, B., Lebrigand, K., Barbry, P., Engelen, S., Lemainque, A., Wincker, P., Liti, G., Schacherer, J.: Genome evolution across 1,011 saccharomyces cerevisiae isolates. Nature **556**(7701), 339–344 (2018). doi:10.1038/s41586-018-0030-5
23. Smukowski Heil, C.S., DeSevo, C.G., Pai, D.A., Tucker, C.M., Hoang, M.L., Dunham, M.J.: Loss of heterozygosity drives adaptation in hybrid yeast. Mol Biol Evol **34**(7), 1596–1612 (2017). doi:10.1093/molbev/msx098
24. Escalona, M., Rocha, S., Posada, D.: A comparison of tools for the simulation of genomic next-generation sequencing data. Nat Rev Genet **17**(8), 459–69 (2016). doi:10.1038/nrg.2016.57
25. Stephens, Z.D., Hudson, M.E., Mainzer, L.S., Taschuk, M., Weber, M.R., Iyer, R.K.: Simulating next-generation sequencing datasets from empirical mutation and sequencing models. PLoS One **11**(11), 0167047 (2016). doi:10.1371/journal.pone.0167047
26. Semeraro, R., Orlandini, V., Magi, A.: Xome-blender: A novel cancer genome simulator. PLoS One **13**(4), 0194472 (2018). doi:10.1371/journal.pone.0194472
27. Laureau, R., Loeillet, S., Salinas, F., Bergström, A., Legoix-Né, P., Liti, G., Nicolas, A.: Extensive recombination of a yeast diploid hybrid through meiotic reversion. PLoS Genet **12**(2), 1005781 (2016). doi:10.1371/journal.pgen.1005781
28. Dutta, A., Lin, G., Pankajam, A.V., Chakraborty, P., Bhat, N., Steinmetz, L.M., Nishant, K.T.: Genome dynamics of hybrid saccharomyces cerevisiae during vegetative and meiotic divisions. G3 (Bethesda) **7**(11), 3669–3679 (2017). doi:10.1534/g3.117.1135
29. Marsit, S., Leducq, J.-B., Durand, É., Marchant, A., Filteau, M., Landry, C.R.: Evolutionary biology through the lens of budding yeast comparative genomics. Nat Rev Genet **18**(10), 581–598 (2017). doi:10.1038/nrg.2017.49
30. Duina, A.A., Miller, M.E., Keeney, J.B.: Budding yeast for budding geneticists: a primer on the saccharomyces cerevisiae model system. Genetics **197**(1), 33–48 (2014). doi:10.1534/genetics.114.163188
31. Magi, A., Tattini, L., Benelli, M., Giusti, B., Abbate, R., Ruffo, S.: Wnp: a novel algorithm for gene products annotation from weighted functional networks. PLoS One **7**(6), 38767 (2012). doi:10.1371/journal.pone.0038767
32. Goffeau, A., Barrell, B.G., Bussey, H., Davis, R.W., Dujon, B., Feldmann, H., Galibert, F., Hoheisel, J.D., Jacq, C., Johnston, M., Louis, E.J., Mewes, H.W., Murakami, Y., Philippsen, P., Tettelin, H., Oliver, S.G..: Life with 6000 genes. Science **274**(5287), 546–567 (1996)
33. Dujon, B.: Yeast evolutionary genomics. Nat Rev Genet **11**(7), 512–24 (2010). doi:10.1038/nrg2811
34. Hittinger, C.T.: Saccharomyces diversity and evolution: a budding model genus. Trends Genet **29**(5), 309–17 (2013). doi:10.1016/j.tig.2013.01.002
35. Marcet-Houben, M., Gabaldón, T.: Beyond the whole-genome duplication: Phylogenetic evidence for an ancient interspecies hybridization in the baker's yeast lineage. PLoS Biol **13**(8), 1002220 (2015). doi:10.1371/journal.pbio.1002220
36. Liti, G., Barton, D.B.H., Louis, E.J.: Sequence diversity, reproductive isolation and species concepts in saccharomyces. Genetics **174**(2), 839–50 (2006). doi:10.1534/genetics.106.062166
37. Lopandic, K.: Saccharomyces interspecies hybrids as model organisms for studying yeast adaptation to stressful environments. Yeast **35**(1), 21–38 (2018). doi:10.1002/yea.3294
38. Mixão, V., Gabaldón, T.: Hybridization and emergence of virulence in opportunistic human yeast pathogens. Yeast **35**(1), 5–20 (2018). doi:10.1002/yea.3242
39. Monerawela, C., Bond, U.: The hybrid genomes of saccharomyces pastorianus: A current perspective. Yeast **35**(1), 39–50 (2018). doi:10.1002/yea.3250
40. Peris, D., Pérez-Torrado, R., Hittinger, C.T., Barrio, E., Querol, A.: On the origins and industrial applications of saccharomyces cerevisiae x saccharomyces kudriavzevii hybrids. Yeast **35**(1), 51–69 (2018). doi:10.1002/yea.3283
41. Liti, G., Carter, D.M., Moses, A.M., Warringer, J., Parts, L., James, S.A., Davey, R.P., Roberts, I.N., Burt, A., Koufopanou, V., Tsai, I.J., Bergman, C.M., Bensasson, D., O'Kelly, M.J.T., van Oudenaarden, A., Barton, D.B.H., Bailes, E., Nguyen, A.N., Jones, M., Quail, M.A., Goodhead, I., Sims, S., Smith, F., Blomberg, A., Durbin, R., Louis, E.J.: Population genomics of domestic and wild yeasts. Nature **458**(7236), 337–41 (2009). doi:10.1038/nature07743
42. Lynch, M., Sung, W., Morris, K., Coffey, N., Landry, C.R., Dopman, E.B., Dickinson, W.J., Okamoto, K., Kulkarni, S., Hartl, D.L., Thomas, W.K.: A genome-wide view of the spectrum of spontaneous mutations in yeast. Proc Natl Acad Sci U S A **105**(27), 9272–7 (2008). doi:10.1073/pnas.0803466105
43. Zhu, Y.O., Siegal, M.L., Hall, D.W., Petrov, D.A.: Precise estimates of mutation rate and spectrum in yeast. Proc Natl Acad Sci U S A **111**(22), 2310–8 (2014). doi:10.1073/pnas.1323011111

44. Nishant, K.T., Wei, W., Mancera, E., Argueso, J.L., Schlattl, A., Delhomme, N., Ma, X., Bustamante, C.D., Korbel, J.O., Gu, Z., Steinmetz, L.M., Alani, E.: The baker's yeast diploid genome is remarkably stable in vegetative growth and meiosis. PLoS Genet **6**(9), 1001109 (2010). doi:10.1371/journal.pgen.1001109
45. Sharp, N.P., Sandell, L., James, C.G., Otto, S.P.: The genome-wide rate and spectrum of spontaneous mutations differ between haploid and diploid yeast. Proc Natl Acad Sci U S A **115**(22), 5046–5055 (2018). doi:10.1073/pnas.1801040115
46. Barrick, J.E., Lenski, R.E.: Genome dynamics during experimental evolution. Nat Rev Genet **14**(12), 827–39 (2013). doi:10.1038/nrg3564
47. Long, A., Liti, G., Luptak, A., Tenaillon, O.: Elucidating the molecular architecture of adaptation via evolve and resequence experiments. Nat Rev Genet **16**(10), 567–82 (2015). doi:10.1038/nrg3937
48. Li, H., Ruan, J., Durbin, R.: Mapping short dna sequencing reads and calling variants using mapping quality scores. Genome Res **18**(11), 1851–8 (2008). doi:10.1101/gr.078212.108
49. Weisenfeld, N.I., Kumar, V., Shah, P., Church, D.M., Jaffe, D.B.: Direct determination of diploid genome sequences. Genome Res **27**(5), 757–767 (2017). doi:10.1101/gr.214874.116
50. Treangen, T.J., Salzberg, S.L.: Repetitive dna and next-generation sequencing: computational challenges and solutions. Nat Rev Genet **13**(1), 36–46 (2011). doi:10.1038/nrg3117
51. Sandmann, S., de Graaf, A.O., Karimi, M., van der Reijden, B.A., Hellström-Lindberg, E., Jansen, J.H., Dugas, M.: Evaluating variant calling tools for non-matched next-generation sequencing data. Sci Rep **7**, 43169 (2017). doi:10.1038/srep43169
52. Pabinger, S., Dander, A., Fischer, M., Snajder, R., Sperk, M., Efremova, M., Krabichler, B., Speicher, M.R., Zschocke, J., Trajanoski, Z.: A survey of tools for variant analysis of next-generation genome sequencing data. Brief Bioinform **15**(2), 256–78 (2014). doi:10.1093/bib/bbs086
53. Li, H.: Toward better understanding of artifacts in variant calling from high-coverage samples. Bioinformatics **30**(20), 2843–51 (2014). doi:10.1093/bioinformatics/btu356
54. Yu, X., Sun, S.: Comparing a few snp calling algorithms using low-coverage sequencing data. BMC Bioinformatics **14**, 274 (2013). doi:10.1186/1471-2105-14-274
55. Rajaby, R., Sung, W.-K.: Transurveyor: an improved database-free algorithm for finding non-reference transpositions in high-throughput sequencing data. Nucleic Acids Res **46**(20), 122 (2018). doi:10.1093/nar/gky685
56. Ghoneim, D.H., Myers, J.R., Tuttle, E., Paciorkowski, A.R.: Comparison of insertion/deletion calling algorithms on human next-generation sequencing data. BMC Res Notes **7**, 864 (2014). doi:10.1186/1756-0500-7-864
57. Marsit, S., Mena, A., Bigey, F., Sauvage, F.-X., Couloux, A., Guy, J., Legras, J.-L., Barrio, E., Dequin, S., Galeote, V.: Evolutionary advantage conferred by an eukaryote-to-eukaryote gene transfer event in wine yeasts. Mol Biol Evol **32**(7), 1695–707 (2015). doi:10.1093/molbev/msv057
58. Huang, M.-E., Rio, A.-G., Nicolas, A., Kolodner, R.D.: A genomewide screen in saccharomyces cerevisiae for genes that suppress the accumulation of mutations. Proc Natl Acad Sci U S A **100**(20), 11529–34 (2003). doi:10.1073/pnas.2035018100
59. Dunham, M.J., Badrane, H., Ferea, T., Adams, J., Brown, P.O., Rosenzweig, F., Botstein, D.: Characteristic genome rearrangements in experimental evolution of saccharomyces cerevisiae. Proc Natl Acad Sci U S A **99**(25), 16144–9 (2002). doi:10.1073/pnas.242624799
60. Dunn, B., Paulish, T., Stanbery, A., Piotrowski, J., Koniges, G., Kroll, E., Louis, E.J., Liti, G., Sherlock, G., Rosenzweig, F.: Recurrent rearrangement during adaptive evolution in an interspecific yeast hybrid suggests a model for rapid introgression. PLoS Genet **9**(3), 1003366 (2013). doi:10.1371/journal.pgen.1003366
61. Gresham, D., Desai, M.M., Tucker, C.M., Jenq, H.T., Pai, D.A., Ward, A., DeSevo, C.G., Botstein, D., Dunham, M.J.: The repertoire and dynamics of evolutionary adaptations to controlled nutrient-limited environments in yeast. PLoS Genet **4**(12), 1000303 (2008). doi:10.1371/journal.pgen.1000303
62. Boeva, V., Zinovyev, A., Bleakley, K., Vert, J.-P., Janoueix-Lerosey, I., Delattre, O., Barillot, E.: Control-free calling of copy number alterations in deep-sequencing data using gc-content normalization. Bioinformatics **27**(2), 268–9 (2011). doi:10.1093/bioinformatics/btq635
63. Tattini, L., D'Aurizio, R., Magi, A.: Detection of genomic structural variants from next-generation sequencing data. Front Bioeng Biotechnol **3**, 92 (2015). doi:10.3389/fbioe.2015.00092
64. Kellis, M., Patterson, N., Endrizzi, M., Birren, B., Lander, E.S.: Sequencing and comparison of yeast species to identify genes and regulatory elements. Nature **423**(6937), 241–54 (2003). doi:10.1038/nature01644
65. Lee, P.S., Greenwell, P.W., Dominska, M., Gawel, M., Hamilton, M., Petes, T.D.: A fine-structure map of spontaneous mitotic crossovers in the yeast saccharomyces cerevisiae. PLoS Genet **5**(3), 1000410 (2009). doi:10.1371/journal.pgen.1000410
66. Gallone, B., Steensels, J., Prahl, T., Soriaga, L., Saels, V., Herrera-Malaver, B., Merlevede, A., Roncoroni, M., Voordeckers, K., Miraglia, L., Teiling, C., Steffy, B., Taylor, M., Schwartz, A., Richardson, T., White, C., Baele, G., Maere, S., Verstrepen, K.J.: Domestication and divergence of saccharomyces cerevisiae beer yeasts. Cell **166**(6), 1397–141016 (2016). doi:10.1016/j.cell.2016.08.020
67. Hallin, J., Märtens, K., Young, A.I., Zackrisson, M., Salinas, F., Parts, L., Warringer, J., Liti, G.: Powerful decomposition of complex traits in a diploid model. Nat Commun **7**, 13311 (2016). doi:10.1038/ncomms13311
68. Li, H., Bloom, J.M., Farjoun, Y., Fleharty, M., Gauthier, L., Neale, B., MacArthur, D.: A synthetic-diploid benchmark for accurate variant-calling evaluation. Nat Methods **15**(8), 595–597 (2018). doi:10.1038/s41592-018-0054-7
69. Kurtz, S., Phillippy, A., Delcher, A.L., Smoot, M., Shumway, M., Antonescu, C., Salzberg, S.L.: Versatile and open software for comparing large genomes. Genome Biol **5**(2), 12 (2004). doi:10.1186/gb-2004-5-2-r12
70. Serero, A., Jubin, C., Loeillet, S., Legoix-Né, P., Nicolas, A.G.: Mutational landscape of yeast mutator strains. Proc Natl Acad Sci U S A **111**(5), 1897–902 (2014). doi:10.1073/pnas.1314423111
71. Okonechnikov, K., Golosova, O., Fursov, M., UGENE team: Unipro ugene: a unified bioinformatics toolkit. Bioinformatics **28**(8), 1166–7 (2012). doi:10.1093/bioinformatics/bts091
72. Walker, B.J., Abeel, T., Shea, T., Priest, M., Abouelliel, A., Sakthikumar, S., Cuomo, C.A., Zeng, Q.,

Wortman, J., Young, S.K., Earl, A.M.: Pilon: an integrated tool for comprehensive microbial variant detection and genome assembly improvement. PLoS One **9**(11), 112963 (2014). doi:10.1371/journal.pone.0112963
73. Li, H., Durbin, R.: Fast and accurate short read alignment with burrows-wheeler transform. Bioinformatics **25**(14), 1754–60 (2009). doi:10.1093/bioinformatics/btp324
74. Li, H.: A statistical framework for snp calling, mutation discovery, association mapping and population genetical parameter estimation from sequencing data. Bioinformatics **27**(21), 2987–93 (2011). doi:10.1093/bioinformatics/btr509
75. Garrison, E., Marth, G.: Haplotype-based variant detection from short-read sequencing (2012). 1207.3907
76. Quinlan, A.R., Hall, I.M.: Bedtools: a flexible suite of utilities for comparing genomic features. Bioinformatics **26**(6), 841–2 (2010). doi:10.1093/bioinformatics/btq033
77. Danecek, P., Auton, A., Abecasis, G., Albers, C.A., Banks, E., DePristo, M.A., Handsaker, R.E., Lunter, G., Marth, G.T., Sherry, S.T., McVean, G., Durbin, R., 1000 Genomes Project Analysis Group: The variant call format and vcftools. Bioinformatics **27**(15), 2156–8 (2011). doi:10.1093/bioinformatics/btr330
78. Li, H.: Tabix: fast retrieval of sequence features from generic tab-delimited files. Bioinformatics **27**(5), 718–9 (2011). doi:10.1093/bioinformatics/btq671
79. Cingolani, P., Platts, A., Wang, L.L., Coon, M., Nguyen, T., Wang, L., Land, S.J., Lu, X., Ruden, D.M.: A program for annotating and predicting the effects of single nucleotide polymorphisms, snpeff: Snps in the genome of drosophila melanogaster strain w1118; iso-2; iso-3. Fly (Austin) **6**(2), 80–92 (2012). doi:10.4161/fly.19695
80. Derrien, T., Estellé, J., Marco Sola, S., Knowles, D.G., Raineri, E., Guigó, R., Ribeca, P.: Fast computation and applications of genome mappability. PLoS One **7**(1), 30377 (2012). doi:10.1371/journal.pone.0030377
81. Robinson, J.T., Thorvaldsdóttir, H., Winckler, W., Guttman, M., Lander, E.S., Getz, G., Mesirov, J.P.: Integrative genomics viewer. Nat Biotechnol **29**(1), 24–6 (2011). doi:10.1038/nbt.1754

Additional Files

Additional file 1 — Supplementary Information
Supplementary figures and text.

Additional file 2 — Table S1. Reads mapping statistics
Statistics of unmapped and MAPQ = 0 reads.

Additional file 3 — Table S2. Variants detected in the A452R14 SK1/BY hybrid and results of the validations
List of the variants detected and validated by means of Sanger sequencing.

Additional file 4 — Table S3. LOHs data in YPS128/DBVPG6765 and N17/DBVPG6765 hybrids
Statistics of the LOHs detected, events detected for all MALs of both hybrids, and legend.

Additional file 5 — Table S4. SNVs data in MALs
Mutation rate statistics and data used for SNVs calculations for all the MALs.

Additional file 6 — Table S5. Indels data in MALs
Mutation rate statistics and data used for indels calculations for all the MALs.

Additional file 7 — Table S6. CNVs data in MALs
Mutation rate statistics and data used for CNVs calculations for all the MALs.

Additional file 8 — LOH segments in all MALs
Images of LOH segments detected in YPS128/DBVPG6765 and N17/DBVPG6765 MALs.

Additional file 9 — Table S8. Number of generations per single-cell bottleneck
The mean number of generations (and the standard deviation) for each MALs used to calculate the mutation rates.

Additional file 10 — Table S9. Mutation rates with mean values and standard deviations
The mean mutation rates and the corresponding standard deviations.

Additional file 11 — Table S10. Coverage statistics
Coverage statistics, after duplicates removal, for all the samples reported in this study.

Figures and Tables

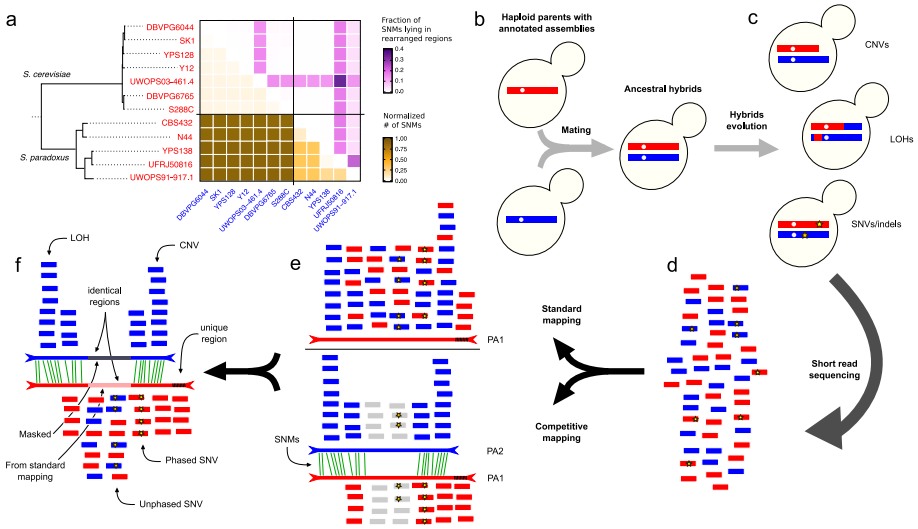

Figure 1 MuLoYDH overview. MuLoYDH comprises: founder parent strains characterization (a), hybrid generation (b) and evolution (c), resequencing of evolved strain (d) and tracking their mutational events (e-f). (a) Complete genome assemblies and annotation guide a rational selection of founder strains with desired genomic distances (bottom left heatmap) and inter-chromosomal rearrangements (top right heatmap). The phylogenetic tree is reproduced from Yue *et al.* [11]. (b) Selected parental strains are combined into ancestral hybrids. The genetic crossing eludes the problems in assembling and phasing diploid genomes. (c) Ancestral hybrids are evolved under different experimental conditions and accumulate different types of *de novo* variants. (d) Genomes from evolved hybrids are sequenced at high coverage by short-read sequencing. (e) Short reads are mapped against the assemblies of the two parental genomes separately (standard mappings) and against the two concatenated assemblies (competitive mapping). For simplicity, standard mapping against only one parental assembly is reported. In the competitive mapping, reads from parent 1 (red) are expected to map to the assembly of parent 1 (PA1) on the basis of the presence of SNMs (green lines). Conversely, reads from parent 2 (blue) are expected to map to the assembly of parent 2 (PA2). Regions bearing no SNM due to high sequence identity are characterized by reads with MAPQ = 0 (light grey reads). (f) Calling small variants from competitive mappings provides direct variant phasing. Regions bearing no SNM are probed for small variants from standard mapping, without direct phasing, against one parental assembly (light red region in PA1), whereas the other one is masked (dark grey segment in PA2). Variants obtained from competitive and standard mappings are combined into a single set of calls.

Table 1 Statistics of SNMs for the constructed hybrids. *S.c.* and *S.p.* refers to *S. cerevisiae* and *S. paradoxus* respectively. For each cross we report: number of SNMs, the genome-wide percentage of SNMs, the fraction of SNMs lying in collinear regions (f_c), fraction of SNMs lying in rearranged regions (f_r) and low-marker-density-regions (LMDRs) fractions. The latter is the fraction of core genomic regions characterized by less than one marker in 300 bp, calculated from pairwise alignment of different pairs of assemblies.

Species	Background	Number of SNMs	SNMs %	f_c	f_r	LMDRs fraction	
						Assembly 1	Assembly 2
S.c./S.c.	SK1/S288C	75547	0.62	0.98	0.02	0.32	0.32
	UWOPS03-461.4/YPS128	63926	0.54	0.81	0.19	0.30	0.31
	YPS128/DBVPG6765	78064	0.66	0.99	0.01	0.24	0.24
S.p./S.c.	N17/DBVPG6765	1095399	9.19	0.96	0.04	0.11	0.11

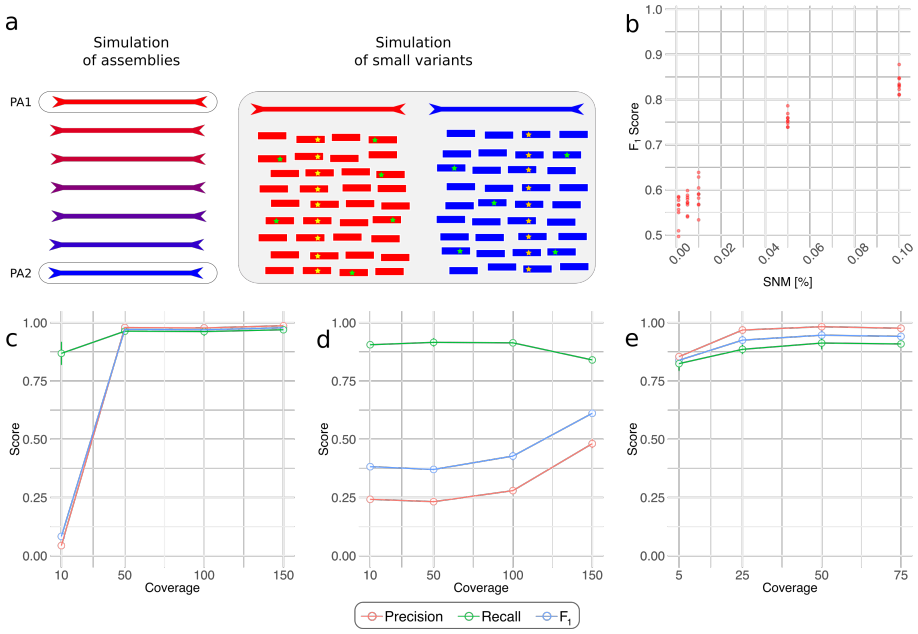

Figure 2 High-accuracy variants detection. (a) Given two assemblies obtained from real data, various levels of heterozygosity are simulated by progressively replacing the polymorphisms of parent 1 (PA1) in the corresponding nucleotides of the assembly of parent 2 (PA2). Small variants (yellow stars) are simulated in known genomic positions to assess the performance of variant calling algorithms from competitive and standard mapping separately with Illumina reads bearing sequencing errors (green stars). (b) The overall performance (F_1 score, see Methods) of small variants detection with competitive mapping decreases with the number of SNMs. For each SNM percentage value, 3 hybrid genomes were simulated from the DBVPG6765/YPS128 hybrid with 3 different replicates of short reads, carrying different variants. The lowest coverage showing F_1 score saturation (25 x, see panel e) was chosen to generate the short-read dataset. (c) DBVPG6044 and YPS128 assemblies are exploited to compare the performance of variant calling using competitive and standard mapping separately. Precision (red), recall (green) and F_1 score (blue) are reported as a function of coverage for: YPS128 complete homozygous diploid data with standard mapping, (d) DBVPG6044/YPS128 heterozygous diploid data with standard mappings against both parental assemblies, and (e) DBVPG6044/YPS128 heterozygous diploid data with competitive mapping. Since we compared the same set of reads in the three approaches, competitive mappings show half of the coverage with respect to standard mappings. Solid lines serve as an eye guide.

Table 2 Mutations rates of different diploid yeast backgrounds. Nuclear mutation rate per generation in different homozygous and heterozygous backgrounds for SNVs, indels, LOHs and CNVs. $\bar{N}_{gen}$ is the average number of generations calculated per single-cell bottleneck. The rates were derived from 8 MALs per background propagated for ∼2250 generations (120 bottlenecks).

Background	$\bar{N}_{gen}$	Mutation rate per generation [bp^{-1}] (Number of variants in 8 lines)			
		SNVs	indels	LOHs	CNVs
YPS128/DBVPG6765	18.7 ± 1.0	$1.49 \cdot 10^{-10}$ (60)	$0.74 \cdot 10^{-11}$ (3)	$2.68 \cdot 10^{-10}$ (114)	$1.17 \cdot 10^{-11}$ (5)
N17/DBVPG6765	18.5 ± 1.3	$2.24 \cdot 10^{-10}$ (89)	$1.00 \cdot 10^{-11}$ (4)	$1.25 \cdot 10^{-10}$ (53)	$0.95 \cdot 10^{-11}$ (4)
DBVPG6765/DBVPG6765	18.6 ± 0.9	$2.82 \cdot 10^{-10}$ (113)	$1.50 \cdot 10^{-11}$ (6)	-	$0.95 \cdot 10^{-11}$ (4)
N17/N17	19.8 ± 0.6	$7.27 \cdot 10^{-11}$ (31)	$4.69 \cdot 10^{-12}$ (2)	-	$2.19 \cdot 10^{-12}$ (1)

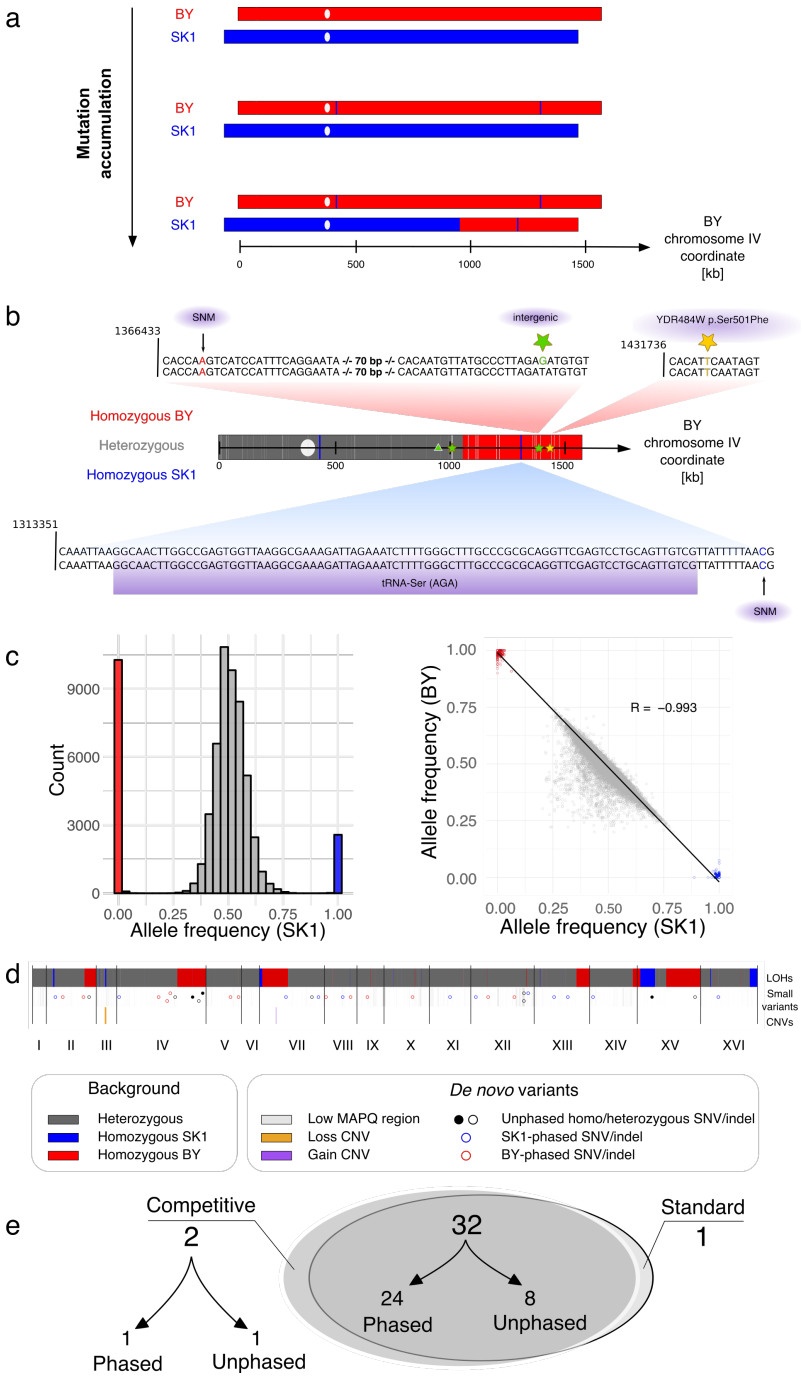

Figure 3 Genome evolution of a mutator hybrid. MuLoYDH provides accurate tracking of the mutational landscape in a SK1/BY *tsa1*Δ/*tsa1*Δ MAL hybrid. (a) Hybrid evolution leads to LOH and (b) to small variants. MuLoYDH performs small variants call on the basis of the LOH regions detected. SNVs and indels are automatically annotated. One homozygous (yellow stars) and one heterozygous (green star) SNVs were detected within LOH regions on chromosomes IV (red: BY, blue: SK1, dark grey: heterozygous segments; white oval: centromere). The presence of SNMs (black arrows) allows direct variant phasing through competitive mapping. A 1-bp deletion was detected in a heterozygous segment and phased to the BY chromosome (green triangle). One heterozygous SNV (green star) was detected from standard mapping (light grey segment). (c) The strategy implemented in MuLoYDH for the detection of LOHs allows noise mitigation (see also Additional file 1: Figure S10) as shown by the clear separation of genotypes with different allele frequencies and by the high negative correlation of allele frequencies. R is the Pearson correlation coefficient. Red (blue) dots/columns refer to homozygous BY (SK1) SNMs, while grey dots/columns refer to heterozygous SNMs. (d) The genome-wide mutational landscape includes CNVs: one gain event in chromosome VII (3 BY copies) and one loss event of the BY allele in chromosome III. (e) Small variants detected from competitive and standard mapping are reported in the Venn diagram. Variants from competitive mapping are classified as phased and unphased. The latter were all detected within LOH regions.

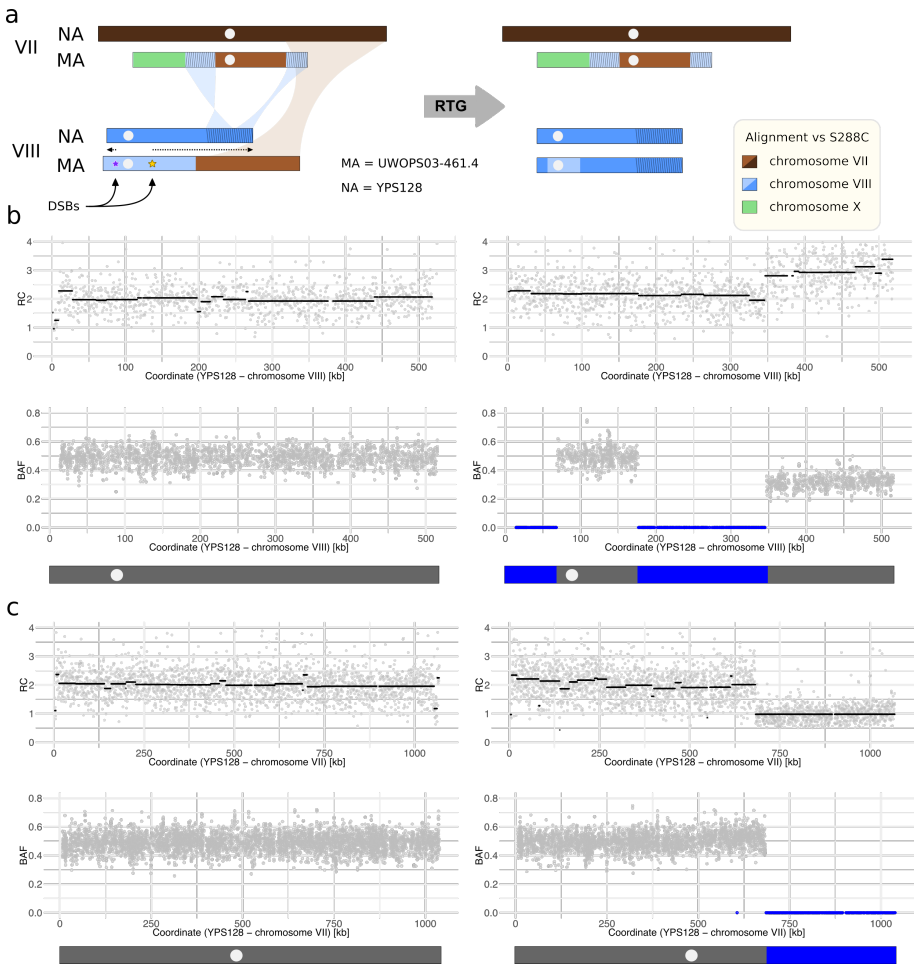

Figure 4 Resolving complex CNVs. (a) Ancestral and RTG-evolved karyotype in a hybrid obtained by crossing UWOPS03-461.4 (a *S. cerevisiae* Malaysian strain, MA) with YPS128 (a *S. cerevisiae* North American strain, NA). Light and dark colors encode for MA and NA alleles respectively. Chromosomal identities were assigned by homologous centromeres. Double-strand breaks in the UWOPS03-461.4 chromosome VIII (purple and yellow stars) were repaired (dotted arrows) using the homologous chromosome from YPS128. These chromosomes bear collinear regions and large inter-chromosomal rearrangements, including a large inversion. Chromosomal identities were determined by centromeres. Repairing a DSB (purple star) in a collinear region with the homologous chromosome leads to a terminal LOH. Repairing a DSB (yellow star) in a chromosome arm bearing collinear and rearranged regions leads to an interstitial LOH and to a complex CNV. (b) Chromosome VIII read count data support the presence of 3 copies of a large segment on the right arm. BAF data from SNMs using mapping against the YPS128 assembly support the presence of a 3-copies region (2 copies of YPS128 and 1 copy of UWOPS03-461.4). The two stretches of BAF values at zero refer to the terminal and interstitial LOH regions (both YPS128 alleles). The former results from DSB repair (purple star, panel a) in chromosome VIII left arm, while the latter is the outcome of DSB repair (yellow star, panel a) in chromosome VIII right arm. (c) Read count signal and BAF data support the deletion of a large segment of UWOPS03-461.4 chromosome VII-R.

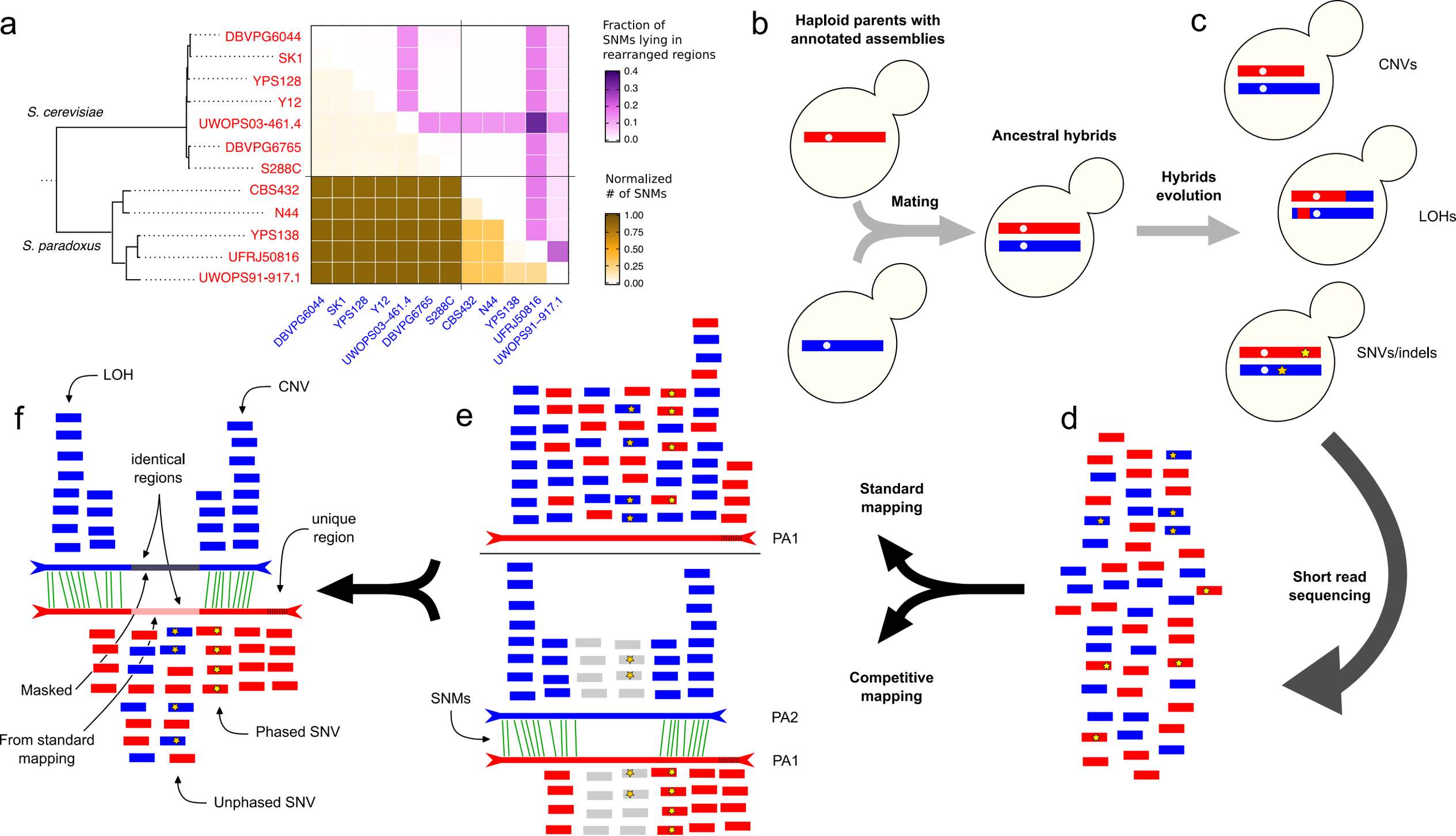
a
DBVPG6044
SK1
YPS128
Y12
UWOPS03-461.4
DBVPG6765
S288C
CBS432
N44
YPS138
UFRJ50816
UWOPS91-917.1
S. cerevisiae
S. paradoxus
Fraction of SNMs lying in rearranged regions
0.4
0.3
0.2
0.1
0.0
Normalized # of SNMs
1.00
0.75
0.50
0.25
0.00
b
Haploid parents with annotated assemblies
Mating
Ancestral hybrids
Hybrids evolution
c
CNVs
LOHs
SNVs/indels
d
Short read sequencing
Standard mapping
Competitive mapping
e
PA1
SNMs
PA2
PA1
f
LOH
CNV
identical regions
unique region
Masked
From standard mapping
Phased SNV
Unphased SNV

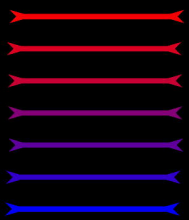

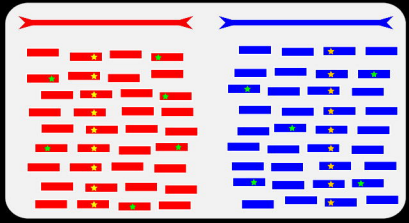

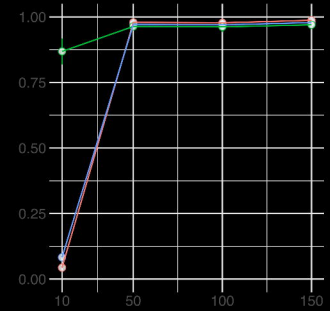
1.00
0.75
0.50
0.25
0.00
10
50
100
150

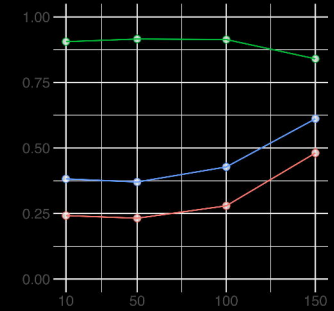
1.00
0.75
0.50
0.25
0.00
10
50
100
150

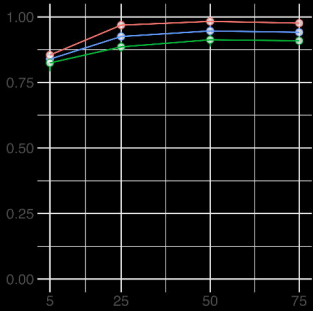
1.00
0.75
0.50
0.25
0.00
5
25
50
75

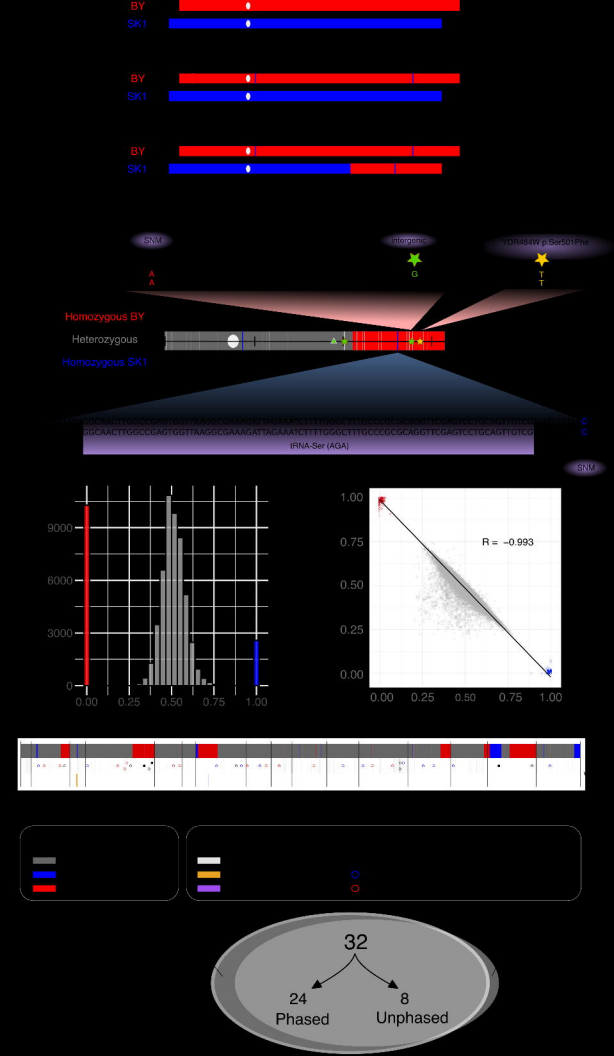
BY
SK1
BY
SK1
BY
SK1
SNV
intergenic
YDR484W p.Ser501Phe
A
A
G
T
T
Homozygous BY
Heterozygous
Homozygous SK1
GGCAACTTGGCCGAGTGGTTAAGGCGAAAGATTAGAAATCTTTTGGGCTTTGCCCGCGGCAGGTTCGAGTCCTGCAGTTTGTCG
tRNA-Ser (AGA)
C
C
SNV
9000
6000
3000
0
0.00
0.25
0.50
0.75
1.00
1.00
0.75
0.50
0.25
0.00
R = −0.993
0.00
0.25
0.50
0.75
1.00
32
24
Phased
8
Unphased

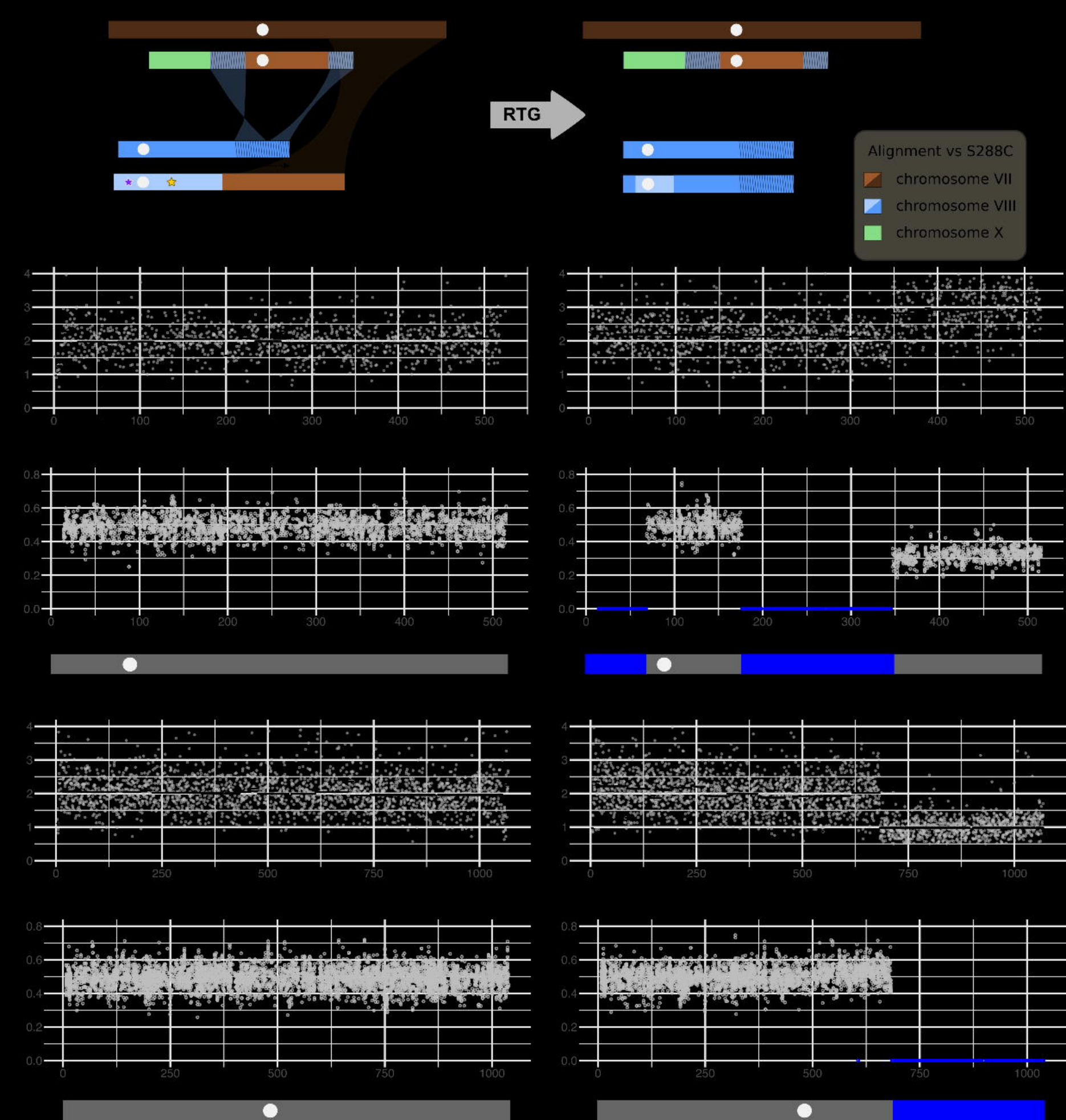
RTG
Alignment vs S288C
chromosome VII
chromosome VIII
chromosome X